Inorg. Chem. **2004**, *43*, 6274–6283

Iron Chelation Properties of an Extracellular Siderophore Exochelin MS

Suraj Dhungana,[†] Colin Ratledge,[‡] and Alvin L. Crumbliss*,[†]

Department of Chemistry, Duke University, Box 90346, Durham, North Carolina 27708-0346, and Department of Biological Sciences, University of Hull, Hull HU6 7RX, UK

Received May 19, 2004

The coordination chemistry of an extracellular siderophore produced by *Mycobacterium smegmatis,* exochelin MS (ExoMS), is reported along with its pK_a values, Fe(III) and Fe(II) chelation constants, and aqueous solution speciation as determined by spectrophotometric and potentiometric titrations. Exochelin MS has three hydroxamic acid groups for Fe(III) chelation and has four additional acidic protons from a carboxylic acid group and three primary amine groups, on the backbone of the molecule. The pK_a values for the three hydroxamic acid moieties, the carboxylic acid group and the alkylammonium groups on ExoMS, correspond well with the literature values for these moieties. Equilibrium constants for proton-dependent Fe(III)–ExoMS equilibria were determined using a model involving the sequential protonation of the Fe(III)–ExoMS complexes at the first and second coordination shells. The equilibrium constants (β) for the overall formation of $Fe(III)ExoMS(H_3)^{2+}$ and $Fe(II)ExoMS(H_3)^{+}$ from $Fe_{(aq)}^{3+}$ or $Fe_{(aq)}^{2+}$ and the deprotonated hydroxamate coordinating group form of the siderophore, $ExoMS(H_3)^{-}$, are calculated as $\log \beta^{III} = 28.9$ and $\log \beta^{II} = 10.1$. A calculated pFe value of 25.0 is very similar to that of other linear trihydroxamic acid siderophores, and indicates that ExoMS is thermodynamically capable of removing Fe(III) from transferrin. The $E_{1/2}$ for the Fe(III)–ExoMS/Fe(II)–ExoMS couple was determined from quasi reversible cyclic voltammograms at pH = 6.5 and found to be –380 mV.

Introduction

Iron is one of the biologically important elements essential for the growth of almost all living organisms. Although iron is the most abundant transition metal in the biosphere, its bioavailability, in aqueous-aerobic conditions and neutral pH, is severely limited due to the formation of insoluble iron hydroxide.[1] The total concentration of soluble iron ($Fe_{(aq)}^{3+} + Fe(OH)_{(aq)}^{2+} + Fe(OH)_{2\ (aq)}^{+}$) at pH = 7.4 and in the absence of chelating ligands is as low as 10^{-10} M.[2,3] At such iron-deficient conditions, direct iron acquisition from the environment becomes very challenging. Higher life forms bypass this challenge by relying on lower life forms for their iron supply; however, organisms at the bottom of the food chain, microorganisms, lack such luxury and are forced to acquire iron directly from the environment.[1]

Microorganisms have developed very specialized iron acquisition and transport systems involving siderophores in order to acquire iron directly from the environment. Siderophores, a class of low-molecular-weight organic molecules, exhibit a high ($\log \beta > 30$) and specific affinity for the Fe^{3+} ion to overcome the solubilization challenge as well as to selectively chelate Fe^{3+} in the presence of other environmentally prevalent metal ions. Under iron-deficient conditions, microbes express siderophore−iron complex specific membrane receptor proteins for efficient assimilation of iron. Cells take up the siderophore−iron complex in an energy-dependent process via these specialized outer membrane receptor proteins. The ability of a microbe to efficiently acquire iron from the environment has proven to be an important virulence factor.[2,4−11]

* Author to whom correspondence should be addressed. E-mail: alc@chem.duke.edu. Fax: (919) 660-1605.
[†] Duke University.
[‡] University of Hull.

(1) Crichton, R. R. *Inorganic Biochemistry of Iron Metabolism: From Molecular Mechanism to Clinical Consequences*, 2nd ed.; Wiley: New York, 2001.
(2) Boukhalfa, H.; Crumbliss, A. L. *BioMetals* **2002**, *15*, 325−339.
(3) Chipperfield, J. R.; Ratledge, C. *BioMetals* **2000**, *13*, 165−168.
(4) Albrecht-Gary, A.-M.; Crumbliss, A. L. In *Metal Ions in Biological Systems*; Sigel, A., Sigel, H., Eds.; Marcel Dekker: New York, 1998; Vol. 35, pp 239−328.
(5) Crumbliss, A. L. In *Handbook of Microbial Iron Chelates*; Winkelmann, G., Eds.; CRC Press: Boca Raton, FL, 1991; pp 177−233.
(6) Matzanke, B. F.; Müller-Matzanke, G.; Raymond, K. N. In *Iron Carriers and Iron Proteins*; Loehr, T. M., Ed.; VCH Publishers: New York, 1989; Vol. 5, pp 3−121.
(7) Neilands, J. B. *J. Biol. Chem.* **1995**, *270*, 26723−26726.

10.1021/ic049343e CCC: $27.50
Published on Web 09/04/2004

Siderophores usually include either hydroxamate or catecholate functional groups for iron coordination,[4,5,8,11] but occasionally, siderophores with new and unusual functional groups, including α-hydroxy carboxylic acid[4,11] and β-hydroxyhistidine,[12−15] have been identified to coordinate iron. The major iron release mechanism from highly stable siderophore−iron complexes is believed to involve reduction of Fe^{3+} to Fe^{2+} and its subsequent transfer to various acceptor molecules within the bacterial cytoplasm;[2,10] however, mechanisms involving ligand exchange, hydrolysis of the siderophore ligand, and/or protonation of the iron−siderophore complex are also believed to be operative.[2,4]

Exochelin MS (Structure **I**) is an extracellular siderophore produced by the nonpathogenic *Mycobacterium smegmatis*.

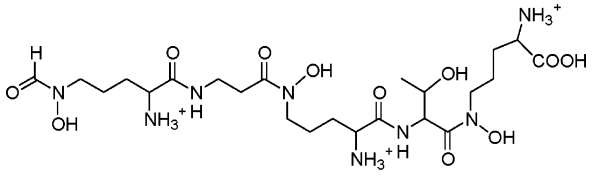

I, Exochelin MS, $H_3ExoMS(H_4)^{3+}$[16]

Mycobacteria, a group that includes the pathogens *Mycobacterium leprae* (cause of leprosy) and *Mycobacterium tuberculosis* (cause of tuberculosis), produce intracellular and extracellular siderophores for iron acquisition and transport. The membrane-associated, intracellular lipophilic siderophores are called mycobactins.[17] The extracellular siderophores are termed either exochelins, for the peptide-based, highly water-soluble molecules, or carboxymycobactins in which the long alkyl chain of mycobactin is replaced with a short acyl chain or a terminally functionalized chain.[18] All mycobactins possess a common core structure and are believed to hold Fe^{3+} within the cell envelope and slowly release it [as Fe^{2+}] through the lipophilic cell membrane.[10,18] The hydrophilic nature of the extracellular exochelins/carboxymycobactins facilitates their sequestration of Fe^{3+}_{aq} from the aqueous-aerobic environment, including host tissues. The extracellular siderophores may transfer Fe^{3+} to the membrane-bound lipophilic mycobactins[10,19,20] or, as in the case of the exochelins, they themselves can act as ligands for the transport of iron through the cell membrane. Saprophytic mycobacteria (including *Mycobacterium smegmatis* and *Mycobacterium neoaurum*) produce and utilize peptide-based exochelins as their primary siderophore for Fe^{3+} acquisition,[12,18,21] while all pathogenic mycobacteria excrete carboxymycobactins as their sole extracellular siderophore.

Exochelin MS is a formylated pentapeptide (*N*-(δ-*N*-formyl, δ*N*-hydroxy-*R*-ornithyl)-β-alaninyl-δ*N*-hydroxy-*R*-ornithinyl-*R*-allo-threoninyl-δ*N*-hydroxy-*S*-ornithine) with three hydroxamic acid groups for Fe^{3+} chelation.[21] The three ornithine residues are connected via their δ-*N*(OH) and α-CO groups, resulting in three free α-NH_2 groups. The presence of two unconventional peptide bonds involving the three *R*(D)-amino acids, unusual in siderophores, make exochelin MS resistant to peptidase hydrolysis. Similar to many known siderophores, exochelin MS has three hydroxamic acid groups for Fe(III) chelation; however, its highly charged backbone sets it apart from conventional trihydroxamic acid siderophores.

A complete solution and thermodynamic characterization of the Fe^{3+}−exochelin MS complex as a function of pH will provide information relevant to the Fe^{3+} acquisition and uptake mechanism in *M. smegmatis* and give insight into the ability of exochelin MS to act as both an extracellular and intracellular siderophore. An in-depth knowledge of such a versatile role of exochelin MS will contribute to a better understanding of the Fe(III) transport pathways in the mycobacteria family.[22] The aqueous solution coordination chemistry of iron with exochelin MS is one of the first examples of such characterization for the exochelin family of siderophores, in addition to a previously studied exochelin MN system.[14] A comparative analysis of the Fe(III) binding properties of these two exochelins, along with knowledge of their Fe(III) uptake capabilities in different biological systems, can provide valuable insight into organism- specific uptake processes and the mechanisms involved. Exochelin MS (**I**) is a linear trihydroxamic acid with a highly charged backbone at physiological pH. A comparative study of the Fe^{3+} coordination properties of exochelin MS with other well-studied linear trihydroxamic acid siderophores with relatively low charged backbones, e.g. ferrioxamine B and ferrioxamine D_1, may help to better define the role of the charged second coordination shell during the Fe^{3+} acquisition and transport processes. This report describes the complete

(8) Raymond, K. N.; Telford, J. R. In *NATO ASI Series C, Mathematical and Physical Sciences*; Kessissoglous, D. P., Eds.; Kluwer Academic Publishers: Dordrecht, The Netherlands, 1995; Vol. 459, pp 25−37.
(9) Winkelmann, G. *Handbook of Microbial Iron Chelates*; CRC Press: Boca Raton, FL, 1991.
(10) Ratledge, C.; Dover, L. G. *Annu. Rev. Microbiol.* **2000**, *54*, 881−941.
(11) Stintzi, A.; Raymond, K. N. In *Molecular and Cellular Iron Transport*; Templeton, D. M., Eds.; Marcel Dekker: New York, 2002; pp 273−320.
(12) Sharman, G. J.; Williams, D. H.; Ewing, D. F.; Ratledge, C. *Chem. Biol.* **1995**, *2*, 553−561.
(13) Dong, L.; Miller, M. J. *J. Org. Chem.* **2002**, *67*, 4759−4770.
(14) Dhungana, S.; Miller, M. J.; Dong, L.; Ratledge, C.; Crumbliss, A. L. *J. Am. Chem. Soc.* **2003**, *125*, 7654−7663.
(15) Hancock, D. K.; Coxon, B.; Wang, S. Y.; White, E. V.; Reeder, D. J.; Bellama, J. M. *J. Chem. Soc., Chem. Commun.* **1993**, 468−469.
(16) Exochelin MS in its fully protonated form is represented by $H_3ExoMN(H_4)^{3+}$ where the "H_3" component represents the three ionizable protons associated with donor groups directly bound to Fe(III) in the first coordination sphere (hydroxamate groups), and the "H_4" components represent the ionizable protons associated with three primary amine groups and a carboxylic acid group not coordinated to Fe(III) in the second coordination sphere. See Scheme 1 for structural elucidation.
(17) Snow, G. A. *Bacteriol. Rev.* **1970**, *34*, 99−125.
(18) Ratledge, C. In *Mycobacteria: Molecular Biology and Virulence*; Ratledge, C., Dale, J., Eds.; Blackwell Science Publishers Ltd.: Oxford, UK, 1999; pp 260−286.
(19) Wheeler, P. R.; Ratledge, C. In *Tuberculosis Pathogenesis, Protection, and Control*; Bloom, B. R., Eds.; American Society of Microbiology: Washington, DC, 1994; p 353.
(20) Ratledge, C. In *Iron Transport in Microbes, Plants and Animals*; Winkelmann, G., van der Helm, D., Neilands, J. B., Eds.; VCH Publishers: Weinheim, 1987; pp 207−221.
(21) Sharman, G. J.; Williams, D. H.; Ewing, D. F.; Ratledge, C. *Biochem. J.* **1995**, *305*, 187−196.
(22) Tsukamura, M. In *The Mycobacteria, A Sourcebook*; Kubica, G. P., Wayne, L. G., Eds.; Marcel Dekker: New York, 1984; Vol. Part B, pp 1339−1359.

aqueous solution characterization of the Fe^{3+} and Fe^{2+} coordination chemistry of exochelin MS over a wide pH range.

Experimental Section

Materials. All solutions were prepared in DI water. All pH measurements were made using an Orion 230 A+ pH/ion meter equipped with an Orion ROSS pH electrode filled with 3 M NaCl solution. The pH of all solutions was adjusted with NaOH or $HClO_4$, accordingly. A stock solution of 2 M $NaClO_4$ was prepared from solid sodium perchlorate hydrate (Aldrich 99+%) and standardized by passing it through a Dowex 50 W-X8 strong acid cation-exchange column in H^+ form. The acid displaced from the column was titrated with standard NaOH solution to the phenolphthalein end point. A 2 M $HClO_4$ stock solution was prepared from concentrated perchloric acid (Fisher 70%) and standardized by titration with standard NaOH solution to the phenolphthalein end point. A Fe(III) perchlorate stock solution (0.1 M) was prepared from recrystallized Fe(III) perchlorate (Aldrich), standardized spectrophotometrically in strong acid[23] and titrimetrically by reduction with Sn(II) and titrated with the primary standard potassium dichromate.[24] Carbonate-free NaOH was prepared by diluting 1 M NaOH with deionized water purged with Ar for 45 min and standardized by titration with standard 0.2 M HCl to the phenolphthalein end point.

Iron-free and iron-bound exochelin MS were isolated and purified following procedures published earlier.[14,21] A ferri−exochelin MS solution was prepared by adding 1 equiv of standardized $Fe(ClO_4)_3$ to desferri−exochelin MS and stirred under Ar for 30 min.

Methods. Electrode Calibration. A glass bulb electrode (Corning high performance) was used for the measurement of pH. The glass electrode was calibrated to read pH according to the classical method.[25] The glass electrode was calibrated twice to read pH in the high and low pH regimes following two distinct calibration techniques. The "classical calibration" technique was used for pH measurements over the pH range 2.2−11. In this pH range the electrode was assumed to have a Nernstian response described by eq 1. The calibration was carried out following a previously described method and the data were refined using the software GLEE[26] to obtain the cell constant, $E°$, and the electrode slope, s, and γ parameter (described in the program GLEE[26]). A fixed value of 13.78 was used for pK_w (in 0.1 M $NaClO_4$).[27] The $[H^+]$ in the solutions was measured as E (mV) and was converted to pH using calibration parameters obtained from GLEE.[26]

$$\text{Nernstian response: } E = E° + s \log[H^+] \quad (1)$$

The pH measurements in strongly acidic conditions (below pH 2.2) were carried out assuming a Nernstian electrode response with junction potential, j, as shown in eq 2. The electrode calibration in this low pH range was carried out using a data analysis Excel worksheet prepared by Gans and O'Sullivan[28] following a previously executed analytical procedure.[29]

Nernstian response with junction potential:

$$E = E° + s \log[H^+] + j[H^+] \quad (2)$$

The electrode response was calibrated in terms of $[H^+]$; the response was measured as E (mV) and was converted to pH using eq 2 and the calibration parameters, $E°$, s, and j.

Potentiometric Measurements. All solutions were purged with Ar prior to titration. Samples (10 mL) were placed in a double-walled titration cell maintained at 25.00 ± 0.05 °C by a circulating constant-temperature bath. A Titronic 96 standard buret was used to carry out conventional potentiometric titration experiments. After each addition of standardized NaOH, UV−vis spectra were recorded using a Cary 100 spectrophotometer. The potentiometric data along with its corresponding spectrophotometric data were analyzed simultaneously using the program HYPERQUAD[30] as it allows for the input of potentiometric and/or spectrophotometric data and the simultaneous treatment of multiple titration curves.

Spectrophotometric Measurements. Two separate and independent spectrophotometric titrations were carried out for mid-pH range and low-pH range. For each titration, UV−visible spectra were recorded using a Cary 100 spectrophotometer. UV−visible spectra of the iron complexes as a function of pH were obtained from a single stock solution. The stock solution was divided into different aliquots and each aliquot was separately used for a spectrophotometric titration. Titrations were carried out in both directions, from low pH to high pH and from high pH to low pH, using a different aliquot of iron complex. After each adjustment of pH using a known volume of standardized acid or base, the solution was allowed to equilibrate for 30 min and its visible spectrum was recorded. Corrections were made for dilution due to the addition of acid and base; data were analyzed using SPECFIT/32[31] software. Since the volume of standardized strong acid or strong base added during the titration was recorded, we were also able to use HYPERQUAD[30] software for the data analysis and the simultaneous treatment of multiple titration curves. The uncertainties in log β and the protonation constants were calculated from the standard deviation. Low pH experiments were necessary to protonate the Fe(III)-complex and to determine the β and the protonation constants for the Fe(III)-complex. Both SPECFIT/32[31] and HYPERQUAD[30] produced values for stability and protonation constants that are in agreement within experimental error.

Competition Experiments with EDTA. In a separate series, spectrophotometric experiments involving Fe(III) competition equilibria with ExoMS and EDTA were carried out over a pH range (5−8). The stock solution of Fe(III)−ExoMS was divided into 16 different aliquots. Each aliquot (3 mL) was allowed to equilibrate with a fixed EDTA concentration at various pH values (pH 5−8) (adjusted using strong acid/base to minimize the change in volume) for a week at 25 °C. No further change in the spectral profile indicated that the system had reached equilibrium. The equilibrium solutions contained 2.6×10^{-4} M Fe(III) and 2.6×10^{-4} M exochelin MS, and 1.3×10^{-3} M EDTA. At the end of a week UV−vis spectra and pH were recorded. Under equilibrium conditions at various pHs there were measurable amounts of reactants and products (Fe(III)−ExoMS, Fe(III)−EDTA, ExoMS, and EDTA) present in solution. These competition equilibrium data were refined

(23) Bastian, R.; Weberling, R.; Palilla, F. *Anal. Chem.* **1956**, *28*, 459−462.
(24) Vogel, A. I. *Quantitative Inorganic Analysis Including Elementary Instrumental Analysis*, 3rd ed.; Longmans, Green and Co., Ltd.: London, 1968.
(25) Martell, A. E.; Motekaitis, R. J. *Determination and Use of Stability Constants*, 2nd ed.; VCH Publishers: New York, 1992.
(26) Gans, P.; O'Sullivan, B. *Talanta* **2000**, *51*, 33−37.
(27) Fischer, R.; Byé, R. *Bull. Soc. Chim. Fr.* **1964**, 2920−2929.
(28) Gans, P.; O'Sullivan, B. *StrongH.xls*; Leeds, U.K., and Berkeley, CA, 1999; http://www.chem.leeds.ac.uk/People/Peter_Gans/_private/strongh.xls.
(29) Johnson, A. R.; O'Sullivan, B.; Raymond, K. N. *Inorg. Chem.* **2000**, *39*, 2652−2660.
(30) Gans, P.; Sabatini, A.; Vacca, A. *Talanta* **1996**, *43*, 1739−1753.
(31) Binstead, R. A.; Jung, B.; Zuberbühler, A. D. *SPECFIT/32 Global Analysis System*, 3.0 ed.; Spectrum Software Associates: Marlborough, MA, 2000.

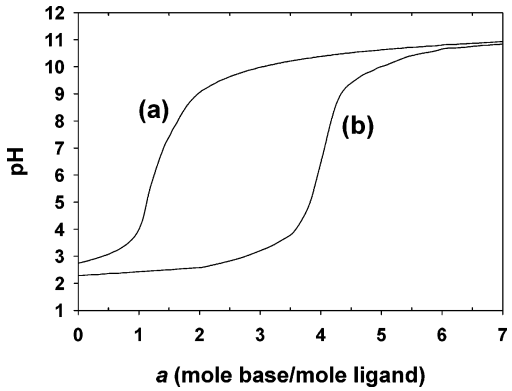

Figure 1. Potentiometric titration curves: (a) 5×10^{-3} M Exochelin MS; (b) Exochelin MS and Fe^{3+}, 1:1, 5×10^{-3} M. Conditions: $T = 298$ K and $\mu = 0.10$ M $NaClO_4$.

Table 1. Ligand pK_a Values for Exochelin MS[a]

n	pK_{an}
1	3.47 ± 0.16
2	7.44 ± 0.12
3	9.29 ± 0.10
4	10.01 ± 0.09
5	10.27 ± 0.08
6	10.99 ± 0.07
7	11.3[b]

[a] Conditions: $T = 298$ K and $\mu = 0.10$ M $NaClO_4$. [b] Estimated for one of the amine groups.

to obtain the overall Fe(III)-binding constant (log β^{III}) for ExoMS using SPECFIT/32 software with a model involving two ligands and a metal.[31] The protonation constants and Fe(III) formation constants for EDTA, and the protonation constants of ExoMS were used as fixed parameters during data analysis. The constants for EDTA were taken from the critical stability constants compilation of Martell and Smith.[32]

Electrochemistry. The electrochemical behavior of the Fe(III)−exochelin MS complex was studied in aqueous solution with 0.1 M $NaClO_4$ as supporting electrolyte at pH = 6.5. The experiment was carried out under Ar atmosphere at room temperature using an EG&G Princeton Applied Research potentiostat model 263. The voltammogram was recorded using PowerCV cyclic voltammetry software at a scan rate of 20 mV/s, with a HDME working electrode, Ag/AgCl (KCl saturated) reference electrode, and platinum wire auxiliary electrode. Potentials referenced to Ag/AgCl (KCl saturated) were converted relative to NHE by adding 197 mV.

Results

Ligand pK_a Constants. Exochelin MS (ExoMS) (**I**) is a hydrophilic extracellular siderophore that easily dissolves in 0.1 M $NaClO_4$ to give a solution of pH 5.92. There are seven different protonation sites on ExoMS: a carboxylic acid group, three hydroxamic acid groups, and three primary amine groups. Six of the seven deprotonation constants were determined by the potentiometric titration of an acidified ExoMS solution. The potentiometric equilibrium curves for free ExoMS and its Fe(III) complex are shown in Figure 1. The deprotonation constants, K_{an} ($n = 1, 2,...7$), for ExoMS are defined by eqs 3 and 4 and are listed in Table 1 as pK_{an} ($-\log(K_{an})$). The acidity of one of the primary amine groups (pK_{a7}) could not be determined, as it is beyond the pH range of our experiments, and an estimated value is listed in Table 1.

$$H_{8-n}ExoMS^{+4-n} \overset{K_{an}}{\rightleftharpoons} H_{7-n}ExoMS^{+3-n} + H^+ \qquad (3)$$

$$K_{an} = \frac{[H_{7-n}ExoMS^{+3-n}][H^+]}{[H_{8-n}ExoMS^{+4-n}]} \qquad (4)$$

The first observed acid dissociation constant for ExoMS, pK_{a1} = 3.47, is assigned to the deprotonation of the carboxylic acid moiety. This proton dissociation constant is slightly lower than that observed for a typical carboxylic acid and is attributed to the α inductive effect of an α amino substitution. The α inductive effect is well established, and is known to lower the pK_a significantly (glutamic acid, a carboxylic acid with α amino substitution, has a pK_a of 2.19, whereas γ carboxyl groups have much higher pK_a values of around 4[33]). The pK_{a2-4} values are assigned to the dissociation of the three hydroxamic acid groups. The pK_{a2} value of 7.44 is slightly lower than normally seen for a hydroxamic acid, while pK_{a3} and pK_{a4} fall in the normal range (pK_a = 8−10) for hydroxamic acids.[34−36] The slightly lowered pK_{a2} value is assigned to the hydroxamic acid group closest to the carboxylate terminal of the molecule and the slight lowering of this pK_a is attributed to the presence of an α amide substitution. The pK_{a3} value of 9.29 is assigned to the middle hydroxamic acid group. The terminal hydroxamic acid group was considered the least acidic of the hydroxamic acid groups and was assigned the pK_{a4} value of 10.01. The fifth (pK_{a5} = 10.27) and sixth (pK_{a6} = 10.99) proton dissociation constants correspond to the deprotonation of the alkylammonium groups and were arbitrarily assigned to the two backbone amine groups. The deprotonation constant corresponding to the terminal amine group adjacent to the carboxylic acid group, pK_{a7}, could not be directly determined and was estimated to be 11.3. This somewhat high estimate takes into consideration possible hydrogen bonding interaction between the amine group and the deprotonated carboxylate group. The pK_a values of all three alkylammoniums are in good agreement with the pK_a values of similar alkylammonium moieties.[32]

Fe(III) Complex Formation and Protonation Constants. General Considerations. The potentiometric titration curve for ExoMS in the presence of an equivalent concentration of Fe(III) is shown in Figure 1. This mid-pH range titration curve shows that three protons, $a = 3$, are very easily released upon Fe(III) binding. The release of these three protons give rise to a buffer region in the lower part of the titration curve. The titration curve exhibits a steady rise beyond $a = 3$ which represents the tight binding of Fe(III). A second buffer region involving three protons is observed at the upper end of the

(32) Martell, A. E.; Smith, R. M. *Critical Stability Constants*; Plenum Press: New York, 2001; Vol. 1.
(33) Fasman, G. D. *Practical Handbook of Biochemistry and Molecular Biology*; CRC Press: Boca Raton, FL, 1989.
(34) Monzyk, B.; Crumbliss, A. L. *J. Org. Chem.* **1980**, *45*, 4670−4675.
(35) Brink, C. P.; Crumbliss, A. L. *J. Org. Chem.* **1982**, *47*, 1171−1176.
(36) Brink, C. P.; Fish, L. L.; Crumbliss, A. L. *J. Org. Chem.* **1985**, *50*, 2277−2281.

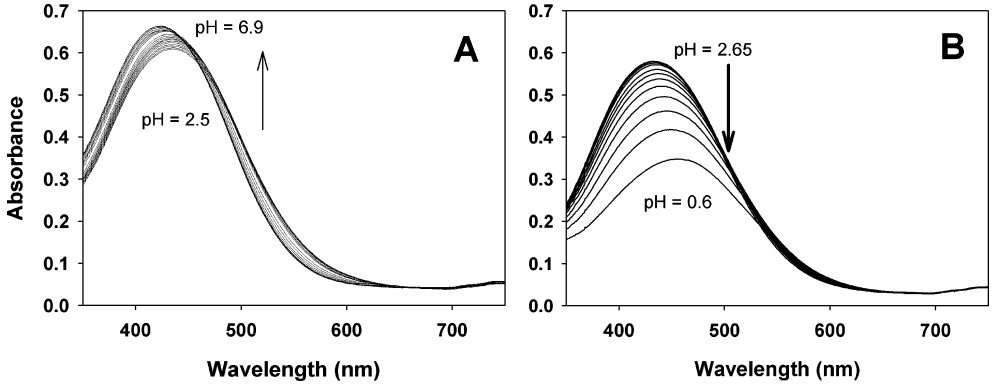

Figure 2. UV-visible spectra of Fe(III)−Exochelin MS as a function of pH: (A) from pH 2.5 to 6.9; (B) from pH 2.65 to 0.6. Conditions: Exochelin MS and Fe^{3+}, 1:1, 2.6×10^{-4} M; $T = 298$ K and $\mu = 0.10$ M $NaClO_4$.

titration curve, beyond $a = 5$. UV−vis absorbance spectra recorded for every point along the potentiometric titration show characteristic ligand-to-metal charge transfer (LMCT) bands for Fe(III)-complexes of hydroxamic acids.[4,5] LMCT bands, $\lambda_{max} = 435$ nm, observed at the beginning of the titration (pH = 2.1) slowly undergo a blue shift as the pH is raised. However, above pH = 5 there was no significant change in the LMCT bands, $\lambda_{max} = 422$ nm ($\epsilon = 2860$ M^{-1} cm^{-1}), indicating the presence of only one Fe(III)−ExoMS species. Above pH = 9 the LMCT band very slowly starts to lose its intensity which is attributed to ligand hydrolysis.

The spectrophotometric titration of ExoMS in the presence of Fe(III) was carried out by monitoring the strong ligand-to-metal charge transfer (LMCT) bands. These titrations were carried out over two distinct pH regimes: mid-pH range (pH >2) and low-pH range (pH <2). The low-pH experiments are important as they include the equilibrium between the fully chelated Fe(III)−ExoMS complex and a protonated form of the Fe(III)−ExoMS complex in which a protonated hydroxamate moiety has dissociated from the Fe(III). In the low pH range the concentration of free proton is much larger compared to the concentration of metal, ligand, and the concentration of protons released due to metal chelation. Therefore, these spectrophotometric data were used to complement the potentiometric data for more accurate measurement of the complexation reactions. The mid-range spectrophotometric experiments show no significant change in the LMCT bands above pH = 5, $\lambda_{max} = 422$ nm ($\epsilon = 2860$ M^{-1} cm^{-1}), indicating the presence of Fe(III) fully coordinated by three hydroxamate moieties. The titration was carried out separately and in both directions, from pH 2.5 to pH 6.9 and from pH 6.9 to pH 2.5, with complete reversibility as indicated by no loss in the intensity of LMCT bands for both sets of experiments. This indicates no significant ligand hydrolysis has occurred over the experimental pH range, which generally results in a loss in the intensity of LMCT bands. A spectral profile for the titration in the mid-pH range is shown in Figure 2A.

The low-pH range experiments were carried out by lowering the pH of Fe(III)−ExoMs solution from pH = 2.65 to pH = 0.6 (Figure 2B). The LMCT band, $\lambda_{max} = 435$ nm, observed at pH 2.65 loses its intensity and undergoes a red shift as the pH of the solution is lowered. At the lowest pH of the spectrophotometric titration (pH = 0.6) the LMCT band with $\lambda_{max} = 455$ nm ($\epsilon = 1710$ M^{-1} cm^{-1}) was observed. This LMCT band is attributed to the bis-hydroxamate Fe(III) complex resulting from protonation and dissociation of a hydroxamate group.

Fe(III)−Exochelin MS Complex Equilibria. A metal−ligand potentiometric titration curve establishes the number of protons involved in the metal−ligand equilibria and the pH range of their involvement. The potentiometric titration for Fe(III)−ExoMS displays a three proton buffer region at low pH range, pH = 2.1−2.5, indicating a relatively easy displacement of the first three protons from ExoMS as the Fe(III)−ExoMS complexation starts (Figure 1). This buffer region also suggests that the pK_as corresponding to successive equilibria liberating three protons lie well below pH = 2.5. The presence of an inflection point at $a = 4$ suggests that a fourth proton is distinctly released during the titration process and the pH value corresponding to $a = 3.5$ (half equivalence point) represents the fourth pK_a for Fe(III)−ExoMS. This pK_a was refined to be 3.37 and is assigned to the acid dissociation of the carboxylic acid group in the second coordination shell of Fe(III) (backbone of the ExoMS molecule and corresponds to pK_{a1} for Fe(III)-free ExoMS; Table 1). The potentiometric titration data refinement, using the program HYPERQUAD,[30] allowed for the calculation of two additional pK_as corresponding to the liberation of the fifth ($a = 5$) and the sixth ($a = 6$) protons. These pK_as were calculated to be 9.24 and 11.17, respectively, and were arbitrarily assigned to the proton dissociations of the two primary alkylammonium moieties present in the second coordination shell of Fe(III) and were found to be similar to the p$K_a$values determined for Fe(III)-free ExoMS. The titration curve between $a = 5$ and $a = 7$ is not steep, which is consistent with proton dissociation taking place in the second coordination shell of Fe(III). The pK_{an} corresponding to the liberation of the seventh ($n = 7$) proton, the terminal amine group, could not be directly determined and was estimated to be 11.3, consistent with our estimation described above for Fe(III)-free ExoMS.

The intense LMCT band of the Fe(III)−ExoMS complex allows the proton-dependent Fe(III)−ExoMS equilibria to be monitored spectrophotometrically. The spectrophotometric titration of the Fe(III)−ExoMS complex (Figure 2A and B)

indicates the presence of two spectroscopically distinguishable forms of Fe(III)−ExoMS over the pH range of the titration (pH = 0.6−6.8). At pH 0.6, the LMCT band displays a λ_{max} at 455 nm ($\epsilon = 1710\ M^{-1}cm^{-1}$). This is characteristic of a bis-hydroxamato-Fe(III) complex[5] and suggests that the Fe(III) complexation by ExoMS occurs at very low pH and further indicates that at a pH as low as 0.6 Fe(III) is already coordinated by two hydroxamate groups. At pH = 5 and above, the Fe(III)−ExoMS complex displays a distinct absorption maximum, $\lambda_{max} = 422$ nm ($\epsilon = 2860\ M^{-1}cm^{-1}$), characteristic of a trishydroxamato-Fe(III) complex[4] and indicates the presence of the second form of Fe(III)−ExoMS in solution. This structural characterization of the Fe(III)−ExoMS complex, involving the coordination of Fe(III) by three hydroxamate groups, is consistent with that seen for other natural and synthetic trihydroxamate siderophores.[4] The spectrophotometric data were analyzed using the program SPECFIT[31] to obtain a pK_a value of 1.2 for the Fe(III)−ExoMS complex. During this spectrophotometric titration the volumes of the strong acid used in the titration were also known, which additionally allowed us to use HYPERQUAD[30] to refine our data and a pK_a value of 1.1 was determined by this analysis. These two techniques produced values that are in agreement with each other within experimental error. This pK_a is assigned to the proton released from the Fe(III)−ExoMS complex when it undergoes conversion from a bishydroxamatodiaquo−Fe(III) to a trishydroxamato−Fe(III) complex. This low pK_a value is in very good agreement with that of ferrioxamine B (0.94), a linear trihydroxamate−Fe(III) complex.[37]

When analyzed together, the complementary potentiometric and spectrophotometric data provide a detailed and more accurate picture of the Fe(III) complexation process by exochelin MS, along with the pK_a values for proton dissociation in the Fe(III)−ExoMS complex at the first and the second coordination shell. These proton dissociation events for Fe(III)−ExoMS can be represented in a generalized form by the stepwise equilibria shown in eqs 5 and 6; the water molecules involved in the equilibria are omitted for simplicity and p$K_n = -\log K_n$. The pK_{1-3} values represent the proton dissociation events at the first coordination shell of Fe(III) and the pK_{4-7} values represent the proton dissociation events at the second coordination shell.[16]

$$\{\text{Fe(III)}-\text{ExoMSH}_{8-n}\}^{+7-n} \overset{K_n}{\rightleftharpoons} \{\text{Fe(III)}-\text{ExoMSH}_{7-n}\}^{+6-n} + \text{H}^+ \quad (5)$$

$$K_n = \frac{[\{\text{Fe(III)}-\text{ExoMSH}_{7-n}\}^{+6-n}][\text{H}^+]}{[\{\text{Fe(III)}-\text{ExoMSH}_{8-n}\}^{+7-n}]} \quad (6)$$

The pK_a values corresponding to the protons released during the Fe(III) complexation process, and the proton dissociation events taking place at the second coordination shell are listed in Table 2.

(37) Schwarzenbach, G.; Schwarzenbach, K. *Helv. Chim. Acta* **1963**, *46*, 1390−1400.

Table 2. pK_a Values and Protonation Constants for the Fe−Exochelin MS Complex[a]

$pK_3 = \log K_{FeHExoMS(H_4)}$	1.2 ± 0.1[b,c]
	1.1 (fixed)[d]
$pK_4 = \log K_{FeExoMS(H_4)}$	3.37 ± 0.12[e]
$pK_5 = \log K_{FeExoMS(H_3)}$	9.24 ± 0.10[e]
$pK_6 = \log K_{FeExoMS(H_2)}$	11.1 ± 0.1[e]
$pK_7 = \log K_{FeExoMS(H)}$	11.3[f]

[a] See Scheme 1 for equilibrium reactions and definition of pK_n and log $K_{FeHxExoMS(Hy)}$. Conditions: $T = 298$ K and $\mu = 0.10$ M $NaClO_4$. [b] Spectrophotometric titration. [c] From SPECFIT/32[31] analysis. [d] From HYPERQUAD[30] analysis. [e] Potentiometric titration. [f] Estimated for the amine group α to the terminal carboxylate group.

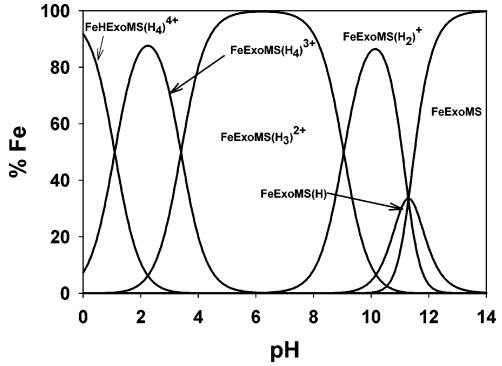

Figure 3. Calculated species distribution for Fe(III) complexes of Exochelin MS. Metal-containing species are normalized to the total concentration of iron. Coordinated water molecules omitted for clarity. Conditions: Exochelin MS + Fe^{3+}, 1:1; $T = 298$ K and $\mu = 0.10$ M $NaClO_4$.

Spectrophotometric titration data indicate that ExoMS starts to coordinate to Fe(III) at a very low pH. At pH = 0.6 two hydroxamate groups are coordinated to Fe(III). The pK_3 value of 1.1 calculated from the spectrophotometric titration is assigned to the proton released from ExoMS as complexation proceeds from a bishydroxamatodiaquo−Fe(III) complex to a trishydroxamato−Fe(III) complex. The first acid dissociation at the second coordination shell involves the release of a proton from the carboxylic acid group. This dissociation constant, pK_4, was determined to be 3.37 and is very similar to the pK_{a1} of the carboxylic acid group in Fe(III)-free ExoMS; thus, in both cases this carboxylic acid group is assumed to behave similarly. The pK_5 and pK_6 values obtained from the potentiometric titration were assigned as the acid dissociation of primary alkylammonium ions (two of the three) present at the second coordination shell of Fe(III). The pK_7 corresponding to the acid dissociation of the terminal alkylammonium moiety (third) within the Fe(III) complex of ExoMS, could not be directly determined and was estimated to be 11.3, consistent with our earlier estimation and based on its lack of interaction with the Fe(III) center.

The potentiometric and spectrophotometric results are summarized in Scheme 1 in the context of Fe(III)−ExoMS complex formation.[16]

Overall Complex Stability and Species Distribution. The pK_a values determined for the Fe(III)−ExoMS complex were used to generate a species distribution plot (Figure 3). The speciation diagram for the Fe(III)−ExoMS system clearly shows hexadentate trishydroxamato−Fe(III) com-

Scheme 1

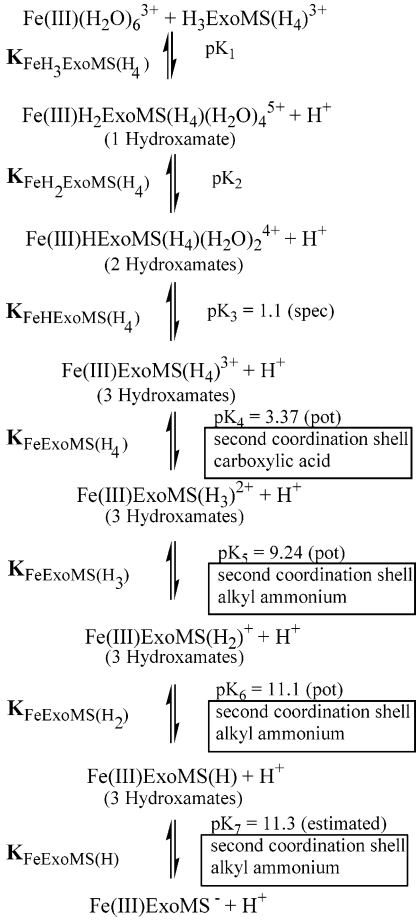

plexes with various degrees of deprotonation in the second coordination shell as the predominant Fe(III)−ExoMS complex over the entire pH range (pH 5−8). At physiological pH, Fe(III)ExoMS$(H_3)^{2+}$ is the only Fe(III)−ExoMS species present in the solution.

The overall stability of the Fe(III) complex of ExoMS (log β^{III}) can be defined by eqs 7 and 8.

$$Fe^{3+}_{(aq)} + ExoMS(H_3)^- \rightleftharpoons Fe(III)ExoMS(H_3)^{2+} \quad (7)$$

$$\beta^{III} = \frac{[Fe(III)ExoMS(H_3)^{2+}]}{[Fe_{(aq)}{}^{3+}][ExoMS(H_3)^-]} \quad (8)$$

This is the usual proton independent stability constant found in compilations of metal−ligand stability constants.[32,38] For the Fe(III)/ExoMS equilibrium system investigated here (and for most other Fe(III)/chelator systems) log β^{III} must be indirectly calculated, since at pH values high enough to produce the donor group deprotonated chelator, ExoMS$(H_3)^-$, $Fe^{3+}_{(aq)}$ will hydrolyze and precipitate. Two methods were used in our study to indirectly calculate log β^{III} for eq 7.

In the first method, spectrophotometric competition experiments with EDTA were performed at various pH values. The competition equilibrium is described by eqs 9 and 10.

$$Fe(III) - ExoMS + EDTA \overset{K}{\rightleftharpoons} Fe(III)EDTA + ExoMS \quad (9)$$

$$K = \frac{[Fe(III)EDTA][ExoMS]}{[Fe(III) - ExoMS][EDTA]} = \frac{\beta^{FeEDTA}}{\beta^{III}} \quad (10)$$

The water molecules and molecular charges involved in the equilibrium are omitted for clarity. The concentrations of Fe(III)−ExoMS were calculated from the absorbance at 422 nm, where Fe(III)−ExoMS is the only light absorbing species. The competition data were used to obtain the overall Fe(III)-binding constant for ExoMS using SPECFIT/32 software with a model involving two ligands and a metal.[31] The stability constant, log β^{III}, for Fe(III)−ExoMS was calculated to be 28.95 (Table 3).

The overall stability constant, log β^{III},[38] for Fe(III)−ExoMS in eqs 7 and 8 was also calculated from the potentiometric and the spectrophotometric data using the software HYPERQUAD[30] and SPECFIT[31] in separate analyses (Table 3). The pK_a values of the carboxylic acid group and the three alkylammonium groups were not included in the calculation of the overall stability as they do not participate in Fe(III) coordination. The log β^{III} calculated for Fe(III)−ExoMS (28.9) is in excellent agreement with the value determined from the EDTA competition experiments within experimental error and comparable to that observed for trihydroxamic-acid-based natural siderophores and siderophore analogues (Table 3).[37,39−43]

The pFe value for ExoMS was calculated (−log[Fe^{3+}] at pH = 7.4 with a total ligand concentration of 10^{-5} M and

Table 3. Fe−Siderophore Complex Thermodynamic Parameters

ligand	log β[a] Fe(III)	log β[a] Fe(II)[c]	pFe[b]	$E_{1/2}$ vs NHE (mV)	ref
Exochelin MS[d]	28.86 ± 0.05[e] 28.92 ± 0.01[f] 28.95 ± 0.11[g]	10.1	25.0	−380	this work
Desferrioxamine B	30.60	10.3	26.6	−468	37, 48−50
Desferrioxamine D_1	30.76		26.45		40
Exochelin MN[d]	39.12 ± 0.17	16.7	31.1	−595	14

[a] Defined as β = [FeL]/[Fe][L] for Fe + L ⇌ FeL (charges omitted for clarity); see ref 38. [b] −log[Fe^{3+}] at $[Fe(III)]_{tot} = 10^{-6}$ M, $[Ligand]_{tot} = 10^{-5}$ M and pH = 7.4. [c] Calculated from eq 11 using E_{aquo} = +732 mV, consistent with previous work from this laboratory (ref 50). [d] Conditions: T = 298 K and μ = 0.10 M $NaClO_4$. [e] From SPECFIT/32[31] analysis using data from spectrophotometric titrations. [f] From HYPERQUAD[30] analysis using data from potentiometric and spectrophotometric titration. [g] EDTA competition experiments as defined in eqs 9 and 10.

(38) β^{III} represents the overall formation constant for Fe(III)-complexes from $Fe_{(aq)}{}^{3+}$ and the donor group deprotonated form of the ligand (for Fe(III)−ExoMS it is the formation of Fe(III)ExoMS$(H_3)^{2+}$, where H_3 represents the total ionizable protons in the second coordination shell). β^{III} reported here can be considered as $\beta_{MLH} = \beta_{110}$ (where M, L, and H represent the metal, ligand, and proton stoichiometry of the complex) for comparative purposes with other data in the literature. β^{II} represents the corresponding formation constant for Fe(II)ExoMS$(H_3)^+$.

(39) Wong, G. B.; Kappel, M. J.; Raymond, K. N.; Matzanke, B.; Winkelmann, G. *J. Am. Chem. Soc.* **1983**, *105*, 810−815.
(40) Anderegg, G.; L'Eplattenier, F.; Schwarzenbach, G. *Helv. Chim. Acta* **1963**, *46*, 1409−1422.
(41) Loomis, L. D.; Raymond, K. N. *Inorg. Chem.* **1991**, *30*, 906−911.
(42) Albrecht-Gary, A.-M.; Blanc, S.; Rochel, N.; Ocaktan, A. Z.; Abdallah, M. A. *Inorg. Chem.* **1994**, *33*, 6391−6402.
(43) Dhungana, S.; Heggemann, S.; Gebhardt, P.; Moellmann, U.; Crumbliss, A. L. *Inorg. Chem.* **2002**, *42*, 42−50.

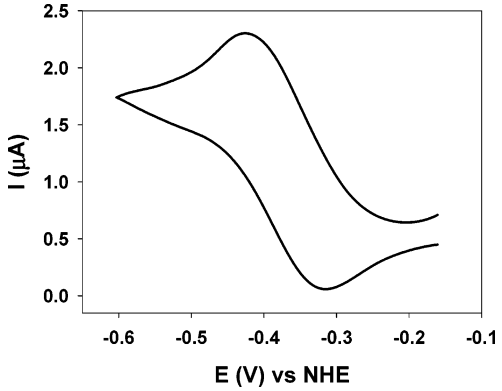

Figure 4. Cyclic voltammogram of Fe(III)−Exochelin MS complex. Conditions: [Fe] = 5×10^{-3} M, [Exochelin MS] = 1×10^{-2} M, pH = 6.5. HDME working electrode, scan rate = 10 mV/s, T = 298 K, and μ = 0.10 M ($NaClO_4$). $E_{1/2}$ = −380 mV(NHE) with a peak separation of 115 mV.

total Fe(III) concentration of 10^{-6} M)[44] to compare the Fe(III) chelating properties of ExoMS with other Fe(III) chelators at physiological conditions. ExoMS was found to have a pFe of 25.0, which is slightly lower than the values calculated for most natural trihydroxamic acid siderophores (Table 3). Nevertheless, this shows a remarkably high affinity of ExoMS for Fe(III).

Electrochemistry and Fe(II) Chelation. The cyclic voltammogram for Fe(III)−ExoMS (Figure 4) corresponding to an Fe(III)/Fe(II) couple displays quasi reversible electrochemistry with a half wave potential ($E_{1/2}$) of −380 mV vs NHE at pH = 6.5. The negative reduction potential for the Fe(III)/Fe(II) couple suggests that ExoMS has a much greater selectivity for Fe(III) over Fe(II). This selectivity is directly reflected in the stability constant of Fe(III) and Fe(II) complexes of ExoMS and is described by eq 11

$$E_{aquo} - E_{complex} = 59.15 \log (\beta^{III}/\beta^{II}) \qquad (11)$$

where β^{III} and β^{II} [38] represent the overall stability constant for the Fe(III) and Fe(II) oxidation states, respectively. The Fe(II)−ExoMS stability constant for ExoMS was calculated using eq 11 and is listed in Table 3.

Discussion

The overall stability of the Fe(III)−ExoMS complex is high, similar to that of other hydroxamate-based natural siderophores and synthetic siderophore analogues (Table 3). The presence of charged residues on the backbone of ExoMS does not seem to have a significant influence on the overall stability of the Fe(III)−ExoMS complex. The proton-dependent equilibrium studies indicate that the Fe(III)−ExoMS complex undergoes successive protonations at both the first and the second coordination shell of Fe(III) with measurable protonation constants for most equilibria. The protonations at the first coordination shell of Fe(III) involve dechelation of the hydroxamate moieties, while protonations at the second coordination shell alter the charge distribution on the backbone of the Fe(III)−ExoMS complex. ExoMS binds Fe(III) very tightly even at low pH, thus only one protonation at the first coordination shell, corresponding to the protonation of a hydroxamate group, could be experimentally observed. This protonation constant (Table 2) was found to be in very good agreement with those calculated for other hydroxamate siderophore systems.[40,45] Second coordination shell protonation occurs at four different sites, a carboxylic acid group and three free primary amine groups on the backbone of ExoMS, and does not affect the chelation/dechelation process. The second coordination shell protonation constants corresponding to the primary amine groups are very similar to those seen for the second coordination shell protonation of free amine groups in other natural siderophores[14,40,45] and are also in good agreement with the protonation constants calculated for ExoMS in the absence of Fe(III) (Table 1).

The stepwise protonation at the second and the first coordination shell of Fe(III) and the dechelation process resulting from first coordination shell protonation are illustrated in Scheme 1 along with the protonation constants, also separately listed in Table 2. The $K_{Fe(III)H_nExoMS(H_n)}$, protonation constants, and pK_a values are related as they describe a protonation and a proton dissociation reaction, respectively, in opposite directions, and a representative relationship is illustrated below.

$$pK_3 = -\log K_3 = -\log(1/K_{Fe(III)HExoMS(H_4)}) = \log K_{Fe(III)HExoMS(H_4)} \qquad (12)$$

The Fe(III)−ExoMS protonation constants influence the species distribution profile as a function of pH (Figure 3) and indicate the relative chelating ability of ExoMS at different pH conditions. The most predominant species at physiologically relevant pH is a trishydroxamato−Fe(III) complex of ExoMS, Fe(III)ExoMS$(H_3)^{2+}$, with a net +2 charge due to the protonated moieties on the ligand backbone. A direct and physiologically relevant comparison of chelator effectiveness is achieved by noting that the pFe of ExoMS is comparable to that of other natural trihydroxamic acid siderophores. The high pFe of ExoMS at physiological pH indicates it is a very effective Fe(III) chelating agent, and coupled with a high hydrophilicity resulting from the net positive charge on the complex, is thermodynamically capable of removing Fe(III) from transferrin.

Our Fe(III)/Fe(II) redox results indicate that the thermodynamic stability of the Fe(II)−ExoMS complex is dramatically decreased compared to that of the Fe(III)−ExoMS complex ($\beta^{II} = 10^{10.1}$; $\beta^{III} = 10^{28.9}$). This decrease in iron affinity in Fe(II)−ExoMS by almost 20 orders of magnitude facilitates the increased lability of the reduced complex with respect to ligand exchange and makes the complex more susceptible to protonation and proton driven dissociation.

The thermodynamic stability of Fe(III)−ExoMS is slightly lower than that of other linear trihydroxamic acid sidero-

(44) Raymond, K. N.; Müller, G.; Matzanke, B. F. In *Topics in Current Chemistry*; Boschke, F. L., Ed.; Springer-Verlag: Berlin, Heidelberg, 1984; Vol. 123, pp 49−102.

(45) Evers, A.; Hancock, R. D.; Martell, A. E.; Motekaitis, R. J. *Inorg. Chem.* **1989**, *28*, 2189−2195.

phores (Table 3), including ferrioxamine B. Exochelin MS and desferrioxamine B are both linear trihydroxamic acids with a terminal protonated amine group (**II**). Over the physiological pH regime, both exochelin MS and desferrioxamine B give rise to hexacoordinated Fe(III) complexes with positive residual charge (2+ and 1+, respectively). Although the net charges on the two complexes differ only by one unit, the number of charged groups on the surface of the Fe(III)−ExoMS complex is significantly higher, which is consistent with the hydrophilic character of this extracellular siderophore. Another major structural difference in the Fe(III) complexes of these two siderophores is the size of the macrocyclic rings (A and B in **II**) that connect two Fe(III) binding moieties. ExoMS has 8 atoms in the macrocyclic ring A and 7 atoms in the macrocyclic ring B, whereas ferrioxamine B has 9 atoms in both rings A and B. The overall Fe(III) affinities of ExoMS ($\beta^{III} = 10^{28.9}$) and desferrioxamine B ($\beta^{III} = 10^{30.6}$),[37] and the first protonation constants for the Fe(III)−ExoMs complex ($10^{1.1}$) and ferrioxamine ($10^{0.94}$),[37] are very close despite this structural difference. This clearly indicates that such a size difference in the macrocyclic ring connecting two Fe(III) binding moieties has relatively little effect on the thermodynamics of Fe(III) binding.

The reduction potential of Fe(III)−ExoMS is more positive than that seen for ferrioxamine B and other linear trihydroxamato−Fe(III) complexes (Table 3). This positive shift suggests a relative ease in the reduction of the Fe(III) center and stabilization of the Fe(II) state. The hydrophilicity of Fe(III)−ExoMS and net positive charge at the pH of investigation may contribute to the observed positive shift in the redox potential of the Fe(III)−ExoMS complex. Thus, in a reduction driven Fe release process, Fe(III)−ExoMS can release Fe more readily than ferrioxamine B, despite their nearly identical thermodynamic affinity for Fe(III). As noted above, reduction results in a decrease in iron binding affinity by almost 20 orders of magnitude, which suggests that Fe(III/II) reduction may be involved in the in vivo release of iron from its ExoMS complex.

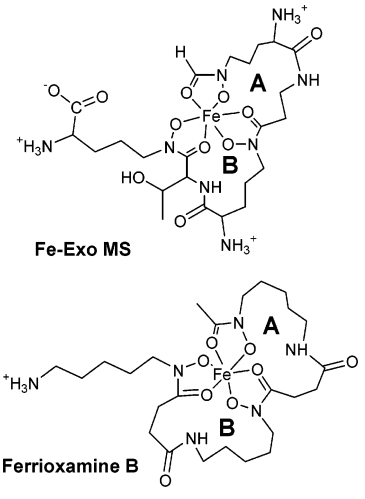

II, Fe(III)-ExoMS and Ferrioxamine B

Exochelin MS belongs to a class of extracellular siderophores produced by mycobacteria for Fe(III) acquisition. The extracellular nature of this siderophore requires it to be hydrophilic at physiological pH. The speciation profile (Figure 3) for Fe(III)−ExoMS clearly indicates that Fe(III)−ExoMS maintains high hydrophilicity by carrying a net positive charge over the physiological pH regime and clearly explains the failure to extract Fe(III)−ExoMS and ExoMN from aqueous solutions using any solvent, including ethanol, from biphasic K_2CO_3 saturated solutions.[21] The exochelin family of siderophores, produced by various mycobacterial species, show significant structural diversity at the Fe(III) coordination site as well as in the overall architecture, while maintaining their hydrophilicity. This structural variation dictates the Fe(III) binding properties of exochelins as well as their specificity for transporting Fe(III) into a narrow range of species; for example, ExoMS is not taken up by *M. neoaurum* but is so by *M. vaccae*, which produces an exochelin similar to that of ExoMS.[46,47] The influence of structural diversity on Fe(III) binding and transport properties of exochelins is certainly pronounced in the case of exochelin MS and exochelin MN (ExoMN, **III**) produced by *M. neoaurum*.[14] Structurally, both exochelins maintain high hydrophilicity at physiological conditions while they drastically differ in their Fe(III) binding groups and consequently in their Fe(III) binding properties (Table 3), thereby helping to explain why neither exochelin can be used by the other organism.[47]

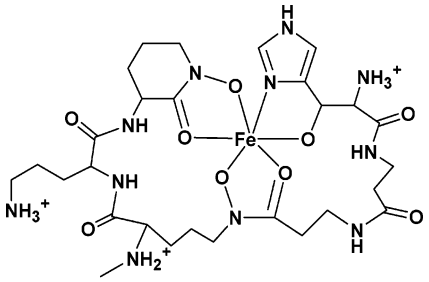

III, Fe(III)-ExoMN

Unlike exochelin MS, exochelin MN binds Fe(III) via an unusual β-hydroxy-L-histidine group, in addition to two hydroxamate groups. Thermodynamic studies of Fe(III)−ExoMN also indicate a unique proton-driven linkage isomerization unique to this siderophore.[14] Although, ExoMS and ExoMN both belong to the same family of extracellular siderophores, exochelins, they display very different Fe(III) binding affinities (Table 3) along with different protonation behavior for their Fe(III)-complexes. Such differences suggest the possibility of different mechanisms of Fe(III) release

(46) Messenger, A. J. M.; Hall, R. M.; Ratledge, C. *J. Gen. Microbiol.* **1986**, *132*, 845−852.
(47) Hall, R. M.; Ratledge, C. *J. Gen. Microbiol.* **1987**, *133*, 193−199.
(48) Bickel, H.; Hall, G. E.; Keller-Schierlein, W.; Prelog, V.; Vischer, E.; Wettstein, A. *Helv. Chim. Acta* **1960**, *43*, 2129−2138.
(49) Cooper, S. R.; McArdle, J. V.; Raymond, K. N. *Proc. Natl. Acad. Sci.* **1978**, *75*, 3551−3554.
(50) Spasojevic, I.; Armstrong, S. K.; Brickman, T. J.; Crumbliss, A. L. *Inorg. Chem.* **1999**, *38*, 449−454.

by these two exochelins. A more positive redox potential for Fe(III)−ExoMS compared to that of Fe(III)−ExoMN also suggests that the Fe(III)−ExoMS complex is more easily reduced and may release Fe in a reduction-driven Fe release process. Over a physiologically relevant pH regime, the Fe(III)−ExoMS complex does not change its first coordination shell; however, the Fe(III)−ExoMN complex undergoes a proton dependent linkage isomerization resulting in the formation of a complex with a vacant coordination site.[14] This vacant coordination site occupied by a water ligand in aqueous media is kinetically labile and may facilitate ligand exchange at the Fe(III) center which may ultimately lead to Fe(III) release from ExoMN. This difference may very well be the feature which allows ExoMN to efficiently facilitate Fe(III) transport into pathogenic *M. leprae* responsible for leprosy, unlike exochelin MS.[12,21,47]

Additionally, the structural differences between these two exochelins and their respective receptor proteins will determine the specificity of the uptake process and make exochelins MS and MN noncompatible for iron uptake in other species. This clearly reestablishes the concept that different mycobacterial species have different Fe(III)-siderophore recognition and transport mechanisms while utilizing the same principle of acquiring Fe(III) from a hydrophilic environment by using highly hydrophilic chelating agents. This structural specificity may be an energetically attractive strategy developed by mycobacterial species to prevent other species from using their exochelin, especially when the synthesis of these chelators is an energy demanding process. However, the ability of pathogenic mycobacteria like *Mycobacterium leprae* (cause of leprosy) to utilize exochelins from other species, e.g., from *M. neoaurum* and also an armadillo-derived mycobacterium which produces an exochelin that can be distinguished from ExoMN,[47] illustrates the versatility of these mycobacteria which can provide a distinct advantage to a pathogen.

Summary and Conclusions

The Fe(III) coordination chemistry of exochelin MS was explored in aqueous solution. The thermodynamic and the spectroscopic properties of the Fe(III) complexes of ExoMS are very similar to those of other trihydroxamic acid siderophores, including ferrioxamine B. The very high Fe(III) binding affinity and pFe of ExoMS is suggestive of an effective chelating agent at physiological conditions, and from a thermodynamic standpoint ExoMS can remove Fe(III) from transferrin. The reduction of Fe(III)−ExoMS to Fe(II)−ExoMS lowers the thermodynamic binding affinity for iron by almost 20 orders of magnitude, and makes the reduced complex more labile with respect to ligand exchange, and more susceptible to protonation and proton-driven iron dissociation. Over the physiological pH range both ExoMS and its Fe(III) complex have a high net positive charge, thus enhancing the hydrophilicity of the siderophore and its iron complex. The structural diversity of the exochelins strongly dictate the Fe(III) binding properties of these hydrophilic extracelluar chelators and may possibly be a key factor in determining their species-specific recognition and transport mechanism.

Acknowledgment. We thank the National Science Foundation (CHE-0079066) for financial support.

IC049343E